A rain-rate retrieval algorithm for attenuated radar measurements

A Rain-Rate Retrieval Algorithm for Attenuated Radar Measurements

PRABHAT K. KONER, ALESSANDRO BATTAGLIA, AND CLEMENS SIMMER

Meteorological Institute, University of Bonn, Bonn, Germany

(Manuscript received 11 May 2009, in final form 15 September 2009)

ABSTRACT

A dynamic regularization scheme for rain-rate retrievals from attenuated radar measurements is presented. Most regularization techniques, including the optimal estimation method, use the state-space parameters to regularize the problem, which will always lead to a bias in the solution. To avoid this problem the authors introduce an evolutionary regularization technique, which is based on the spatial derivative of the measured reflectivity profile and allows for a bias-free global solution. The regularization strength is determined by the quadratic eigenvalue solution using the regularized total least squares method. With the new method, the authors perform a retrieval of rain-rate profiles from simulated measurements of a nadir-pointing W-band (94 GHz) radar, in a configuration similar to the cloud radar employed on *CloudSat*. The simulations assume that multiple scattering is negligible and only liquid hydrometeors are taken into account. The authors compare the results of this method with the outcome of an optimal estimation method and demonstrate that their method is superior in terms of reliability, correlation coefficient, and dispersion to the optimal estimation method for layers experiencing high values of attenuation; therefore, the a priori bias typical for optimal estimation solutions is avoided.

1. Introduction

Spaceborne radars have shown great potential for providing the vertical structure of cloud and precipitation fields over the whole planet. This has been demonstrated by the 14-GHz precipitation radar on board the Tropical Rainfall Measuring Mission (TRMM) satellite, which has been in orbit since November 1997, and more recently by the cloud profiling radar (CPR) on board *CloudSat*, which has been in orbit since June 2006. Although the *CloudSat* mission is devoted primarily to nonprecipitating cloud studies, the CPR is also capable of resolving many precipitation systems. This finding spurred interest in assessing the potential of high-frequency radars for rain retrievals, especially in view of the upcoming global precipitation measurement–European Space Agency Earth Clouds, Aerosols, and Radiation Explorer (GPM–EarthCARE) missions, which will deploy on board both Ka- and W-band radars, and of the current deployments of ground-based cloud radars.

It is well known that the attenuation of radar signals dramatically increases with frequency, whereas the variability of nonattenuated reflectivity diminishes as resonance-scattering effects become more pronounced (Lhermitte 1987). The attenuation issue engenders two major drawbacks: it drives the reflectivity signal below the detectability threshold in the presence of strong rain, and it causes problems in the reconstruction of the attenuation-corrected reflectivity profile itself. Usually, radar retrieval algorithms make extensive assumptions about the structure of drop-size distributions (DSDs) in order to obtain relations of the form $Z = aR^b$ and $k = \alpha R^\beta$, which are directly invertible to rain rates R given radar reflectivity measurements Z. Measured reflectivity can in principle be corrected for the attenuation effects by successively correcting bins, starting either close to the radar (forward Hitchfeld–Bordan method) or at the far side (backward Hitchfeld–Bordan method; Hitschfeld and Bordan 1954). The latter method requires the knowledge of the true reflectivity at the most distant location, which, for example, can be estimated from the path-integrated attenuation (PIA) method (description to follow). The forward method, on the other hand, is inherently unstable and almost nonfunctional for the strongly attenuated radars of interest here. The almost linear dependence between rain intensity and signal

Corresponding author address: Prabhat K. Koner, Meteorological Institute, University of Bonn, Auf dem Huegel 20, D-53121 Bonn, Germany.
E-mail: koner@dal.ca

DOI: 10.1175/2009JAMC2279.1

attenuation can be exploited in statistical attenuation-based estimation methods such as those recently proposed by Matrosov (Matrosov 2005, 2007; Matrosov et al. 2006, 2008). The main weakness of their method is the assumption of vertically constant rain profiles for layer depths of 1 km, which may be useful for stratiform rain events only. However, the slope of the vertical reflectivity profiles, solely in terms of attenuation effects, will intrinsically preclude natural vertical variability for other rain events, especially for hurricanes.

Another approach to avoid the cumbersome parameterizations of the previously mentioned methods is the optimal estimation method (OEM; Rodgers 2000). OEM accounts for uncertainties in both the algorithm assumptions and the true information content of the measurements in a statistically sound approach. The disadvantage of OEM, however, is the dependence of the quality of the retrieved state vector—and of the convergence procedure itself—on the selection of the a priori vector; the solution is always biased toward the a priori. Although this can be beneficial in cases when a priori and actual measurement are of comparable quality, the bias can be detrimental when climatological states are used for the a priori because of the large variability between the states. Especially for precipitation profiles, it is extremely challenging or even impossible to suggest valid a priori and a fortiori profiles for the accompanying covariance matrices. In these situations, the structure of the a priori might have little in common with the true profile. It is a common argument that a priori information tends to force the solution into proper behavior; however, very general a priori information will just introduce another source of error into the solution, as we will show.

These drawbacks of the OEM are generally met when profiling rain intensity with high frequency—that is, W-band, radars. L'Ecuyer and Stephens (2002) underlined this difficulty for rain rates above 1.5 mm h^{-1} and pointed to the need for additional information such as PIA, derived from the surface reference technique, or the precipitation water path, estimated from collocated passive microwave radiometers to constrain the retrieval. With this additional information available, accurate, quantitative rainfall estimates can be made at 94 GHz, provided the near-surface rain rate does not exceed 10 mm h^{-1}.

An alternative approach is a deterministic inversion, which also helps us to better understand the general retrieval problem. The deterministic retrieval problem requires the true inverse solution of the radiative transfer equation (RTE). For attenuating radars the RTE is nonlinear and the retrieval is inherently mathematically ill posed. The iterative regularization methods are most popular for solving nonlinear ill-posed inversion problems (Sun et al. 2007; Veselovskii et al. 2002; Su et al. 2007; Demoment 1989; Doicu et al. 2003, 2004; Ceccherini 2005; Hohage 1997; Steck and Clarmann 2001; Deufhard et al. 1998; Hanke 1997; Riddell et al. 2002; Steck 2002). Regularization usually appears mathematically in the form of penalty terms, which constrain the solution according to the characteristics of the stabilizer (Koner and Drummond 2008b; Tsai and Kao 2006). These stabilizers are generally constructed based on state-space parameters, which easily introduce biases and regularization errors into the retrievals. To avoid this problem, we introduce a new, evolutionary stabilizer based on the spatial derivative of the measurement.

One of the difficulties for any regularization method in a nonlinear inverse problem is the optimal weighting of the penalty term as a trade-off between the error and the spatial structure (resolution) of the solution (Vasco 1997; Ceccherini 2005). The discrete L-curve method is popular for determining the value of the regularization parameter in iterative regularization methods; here, a compromise is made between the minimization of the constraints and the minimization of the differences between the measured and simulated spectra weighted by the noise (Hansen 1998; Schimpf and Schreier 1997). However, the discrete L-curve method also has some drawbacks (Rodriguez 2005): there are unexpected oscillations near the corners, false corners, and the loss of convexity, which leads to an inaccurate estimate of the regularization parameter. Moreover, for severely ill-conditioned and nonlinear problems, the discrete L-curve totally loses its "L" shape and the selection of an approximate regularization parameter becomes difficult. To solve this problem, we propose the regularized total least squares (RTLS) method. The RTLS determines the regularization strength using the error criteria implicitly (VanHuffel and Vandewalle 1991; Sima et al. 2004; Markovsky and VanHuffel 2007). In the following, we present an approach to solve the attenuated radar retrieval problem based on a new dynamic regularization scheme (DRS). Both the stabilizer and the regularization strength are constructed using the measurement space parameters dynamically.

2. Mathematical background

Physicists usually develop mathematical models from physical considerations; however, the solution of a model often diverges from the intended physics. The intermediate steps of a long calculation may not have a simple physical meaning nor grant physical insight. For example, the retrieval error involved in an ill-conditioned inversion hinges not only on the measurement noise but also

depends on errors associated with the forward modeling, the Jacobian error, the discretization error, the nonlinearity errors, and/or the numerical noise. The estimation of these methodology errors, that is, errors related to the forward model, is practically impossible. Even a good estimate of the measurement noise is often extremely challenging. If the problem is ill conditioned, however, such errors are amplified in each iteration because of the condition number of the Jacobian (see definition to follow). We will demonstrate this in our study as a specific example of how the error in the Jacobian feeds back to the retrieval solution error, even in a simple linear inversion scheme. Jacobians always have an error (especially in scattering radiative transfer problems) because they are evaluated by finite-difference techniques, with no analytical expression being available. To elucidate the problem, we assume a generalized linear equation of

$$\mathbf{y} = \mathbf{J}\mathbf{x}, \tag{1}$$

where $\mathbf{y}$ is the measurement vector, $\mathbf{J}$ is a matrix, and $\mathbf{x}$ is the state vector. In this formulation, $\mathbf{J}$ is a linearized version of the forward operator—that is, the Jacobian of the RTE. The exact solution of Eq. (1) is $\mathbf{x} = \mathbf{J}^{-1}\mathbf{y}$, which only exists, however, when $\mathbf{J}$ is nonsingular. If we assume that $\mathbf{x} + \delta\mathbf{x}_{\mathrm{rtv}}$ is the exact solution for $\mathbf{J}_h = \mathbf{J} + \delta\mathbf{J}$, where δJ is the error in the Jacobian, we have to rewrite so that

$$(\mathbf{J} + \delta\mathbf{J})(\mathbf{x} + \delta\mathbf{x}_{\mathrm{rtv}}) = \mathbf{y}. \tag{2}$$

If we drop the double-order term and replace $\mathbf{y}$ by $\mathbf{y} = \mathbf{J}\mathbf{x}$, we may write that

$$\delta\mathbf{x}_{\mathrm{rtv}} = \mathbf{J}^{-1}\delta\mathbf{J}\,\mathbf{x}. \tag{3}$$

With $\|\cdot\|$, the l_2 vector norm (which for a square matrix corresponds to the absolute value of the largest eigenvalue) becomes

$$\|\delta\mathbf{x}_{\mathrm{rtv}}\| \le \|\mathbf{J}^{-1}\|\|\delta\mathbf{J}\|\|\mathbf{x}\|. \tag{4}$$

Here, Eq. (4) can be rewritten by multiplying the right-hand side by $\|\mathbf{J}\|/\|\mathbf{J}\|$ and dividing both sides by $\|\mathbf{x}\|$:

$$\frac{\|\delta\mathbf{x}_{\mathrm{rtv}}\|}{\|\mathbf{x}\|} \le \|\mathbf{J}^{-1}\|\|\mathbf{J}\|\frac{\|\delta\mathbf{J}\|}{\|\mathbf{J}\|}. \tag{5}$$

By definition the condition number of the matrix $\mathbf{J}$ is given by $\kappa(\mathbf{J}) = \|\mathbf{J}^{-1}\| \times \|\mathbf{J}\|$. Assuming the $\mathbf{x}$ and $\mathbf{J}$ spaces to be normalized, it can be shown that

$$\|\delta\mathbf{x}_{\mathrm{rtv}}\| \le \kappa(\mathbf{J})\|\delta\mathbf{J}\|. \tag{6}$$

This implies that the retrieval relative error resulting from the error in the Jacobian is enhanced by the condition number of the Jacobian. For example, in the presence of a relative Jacobian error of 10^{-6}, a condition number of the Jacobian equal to 10^7 may introduce more than a 100% error into the retrieval, solely for the Jacobian error. A well-conditioned matrix has a condition number of around 1; a matrix is ill conditioned when the condition number is much greater than 1. We can tentatively classify the ill-conditioned matrices as moderately ill conditioned $1 < \kappa(\mathbf{J}) < 10^2$, highly ill conditioned $10^2 < \kappa(\mathbf{J}) < 10^8$, and severely ill conditioned $10^8 < \kappa(\mathbf{J}) < 10^{16}$. Matrices are rank deficient when $\kappa(\mathbf{J}) > 10^{16}$ in a double-precision calculation. The same relation between the measurement error and the condition number of a Jacobian is reported (Koner and Drummond 2008b; Danzer et al. 2004; Gabella et al. 1997). This approach can be extended to all types of errors in an ill-posed inversion (the derivations are not shown here), and a generalized equation can be formulated by assuming an additive nature of the errors:

$$\|\delta\mathbf{x}_{\mathrm{rtv}}\| \le \kappa(\mathbf{J})\sum_{i=1}^{n}\|\delta\mathbf{E}_i\|, \tag{7}$$

with $\delta\mathbf{E}_i$, $i = 1, 2, \ldots, n$ for the different errors. For example, $\delta\mathbf{E}_1 \rightarrow \delta\mathbf{y}$ is the measurement error, $\delta\mathbf{E}_2 \rightarrow \delta\mathbf{J}$ is the Jacobian error, $\delta\mathbf{E}_3 \rightarrow \delta\boldsymbol{\eta}$ is the nonlinearity error, $\delta\mathbf{E}_4 \rightarrow \delta\boldsymbol{\chi}$ is the discretization error, $\delta\mathbf{E}_5 \rightarrow \delta\boldsymbol{\phi}$ is the numerical noises, and so on.

From mathematics, the condition number of the Jacobian is the main source of the error propagation from the measurement space and inversion space to the state space and may yield an unacceptable solution. Thus the reduction of the condition number of the Jacobian for a Jacobian-based ill-conditioned inversion problem is of utmost importance. The reduction of the condition number of the Jacobian can be achieved by introducing additional constraints (or information). This kind of regularization should not be mixed up with other methods for solving these problems—for example, like the Tikhonov regularization techniques. For the latter techniques, the solution will contain the regularization error and bias according to the characteristics of the stabilizer because the applied mathematical/statistical constraints are based on the state-space parameters. In our approach, which will be discussed in more detail in section 3a, the reduction of the condition number of the Jacobian is the main target and we use the spatial derivative of the measurement instead. Thus, our method does not approximate the solution. More detailed discussions

about regularization in ill-conditioned inversions can be found in Schimpf and Schreier (1997) and Koner and Drummond (2008b).

An important issue is to find the optimal regularization strength, which is dependent on the degree of ill condition of the Jacobian and the error associated to the problem. Many Jacobian-based techniques determine the regularization strength using only the measurement error. There are, however, many other errors and some of these are virtually impossible to estimate as discussed previously. Thus, we use the RTLS method, which implicitly considers most errors for the determination of the regularization strength automatically (see section 3b).

3. Dynamic regularization scheme

The unconstrained optimization related to the regularization of an ill-conditioned Jacobian, given a set of unknowns $\mathbf{x}$, and measurements [$\mathbf{y}_\delta(\mathbf{y}_\delta = \mathbf{y} + \delta\mathbf{y})$, $\delta\mathbf{y}$ of measurement error] can be formulated as (Wang and Yuan 2005)

$$\min_{\mathbf{x}\in\mathbf{X}} \Im_\alpha(\mathbf{x}, \mathbf{y}) \equiv \|\mathbf{y}_\delta - f(\mathbf{x})\|^{\mathrm{T}} \|\mathbf{y}_\delta - f(\mathbf{x})\| + \alpha \mathbf{x}^{\mathrm{T}} \mathbf{R} \mathbf{x}, \quad (8)$$

where, $\mathbf{L}^{\mathrm{T}}\mathbf{L} = \mathbf{R}$ serves as the stabilizer, $\mathbf{L}$ is the regularization operator, $\mathbf{y}_\delta - f(\mathbf{x})$ is the object function, α is the regularization strength, and $\Im_\alpha(\mathbf{x}, \mathbf{y})$ is the cost function. The first-order necessary condition for an optimum solution for x in our algorithm can be formulated by taking a derivative of Eq. (8) so that

$$\mathbf{J}(\mathbf{x})[\mathbf{y}_\delta - f(\mathbf{x})] + \alpha \mathbf{R}\mathbf{x} = 0, \quad (9)$$

where, $\mathbf{J}(\mathbf{x})$ is the Jacobian of the vector object function $\mathbf{y}_\delta - f(\mathbf{x})$. The above formulation is not yet suitable for numerical computation because of the nonlinearity of the vector object function. The necessary linearization can be done by using a Taylor series expansion. The problem is then solved by iteratively using a linear inversion of the Taylor series expansion. Thus the minimization at the kth iteration $\mathbf{x}_k$ becomes

$$\min_{\mathbf{S}_k\in\mathbf{X}} \Im_\alpha(\mathbf{S}_k, \mathbf{y}) \equiv \frac{1}{2}[\|\mathbf{y}_\delta - f(\mathbf{x}_k) - \mathbf{J}(\mathbf{x}_k)\mathbf{S}_k\|^2 + \alpha\|\mathbf{L}\mathbf{S}_k\|^2], \quad (10)$$

with $\mathbf{S}_k = \mathbf{x}_{k+1} - \mathbf{x}_k$ as the step size in a search direction. The main steps of the current algorithm at the kth iteration is as follows:

1) Input $\mathbf{x}_{k-1}$ and $\mathbf{y}_\delta$.
2) Develop the finite-difference Jacobian $\mathbf{J}$, based on the $\mathbf{x}_{k-1}$ and the forward model.
3) Develop the evolutionary operator $\mathbf{L}$, using the height derivative of the measurement (this will be discussed explicitly in section 3a).
4) Calculate the optimal regularization strength, using the RTLS method (this will be discussed in section 3b).
5) Calculate the step size in a search direction using Eq. (10) as

$$\mathbf{S}_k(\mathbf{x}_{k-1}) = (\mathbf{J}^{\mathrm{T}}\mathbf{J} + \alpha\mathbf{L}^{\mathrm{T}}\mathbf{L})^{-1}\mathbf{J}^{\mathrm{T}}[\mathbf{J}\mathbf{x}_{k-1} - \mathbf{y}_\delta + f(\mathbf{x}_{k-1})] - \mathbf{x}_{k-1}. \quad (11)$$

6) Update the state-space parameter following the equation $\mathbf{x}_k = \mathbf{x}_{k-1} + \mathbf{S}_k$.
7) Calculate the regularized gradient using Eq. (9) and Eq. (10) for the convergence check:

$$\mathbf{G}_r(\mathbf{x}_{k-1}) = \left\langle \begin{bmatrix} \mathbf{J} \\ \sqrt{\alpha}\mathbf{L} \end{bmatrix}^{\mathrm{T}} \mathbf{S}_k \right\rangle^{\mathrm{T}} \left\langle \begin{bmatrix} \mathbf{J} \\ \sqrt{\alpha}\mathbf{L} \end{bmatrix}^{\mathrm{T}} \mathbf{S}_k \right\rangle = \mathbf{S}_k^{\mathrm{T}}(\mathbf{J}\mathbf{J}^{\mathrm{T}} + \alpha\mathbf{L}\mathbf{L}^{\mathrm{T}})\mathbf{S}_k. \quad (12)$$

The convergence criterion is based on the familiar condition for a smooth function to achieve a minimum—that is, its gradient must be zero. Regularization is a must when the problem is ill conditioned, like for the present case. There is also the danger of creating a systematic error resulting from noise, as we will discuss later. The condition for convergence for the current problem is to set $\mathbf{G}_r(\mathbf{x}_{k-1}) \ll \varepsilon n$. Here, n is the number of state-space parameters and the default value of 10^{-3} for ε is selected. The previous convergence criterion sometimes may not be sufficient for a highly ill-posed and noisy system because of the numerical instability. Thus, we have added the following additional criteria to terminate the iterative loop: 1) a limited number of iterations, 2) when the update of the value in search direction ($\mathbf{S}_k^{\mathrm{T}}\mathbf{S}_k$) is very low, and 3) when the residual is less than the expected noise $|\delta|$.

The DRS method presented here, dynamically constructs the regularization operator at each iteration step based on the height derivative of the object function. The regularization strength and the Jacobian matrix are also evaluated at each iteration step.

a. Evolutionary regularization operator

The minimization problem of Eq. (10) can be expressed in an alternative form as

$$\mathbf{J}(\mathbf{x}_{\mathrm{true}} - \mathbf{x}_k) = \mathbf{y}_\delta - f(\mathbf{x}_k) \quad \text{and} \quad \sqrt{\alpha}\mathbf{L}(\mathbf{x}_{\mathrm{true}} - \mathbf{x}_k) = 0, \quad (13)$$

with $\mathbf{x}_{\text{true}}$ *and* $\mathbf{x}_k$ as the true value and the retrieved value at the kth iteration of the state-space parameters, respectively. Conventionally, $\mathbf{L}$ is assumed to be a first- or second-derivative operator, which minimizes the adjacent state-space parameters. In such a formulation, it is assumed that the right-hand side of the regularization part of Eq. (13) is zero, which is, however, not exactly true. For instance, there will be a regularization error if the true profile is not constant for the first-derivative operator and if the true profile is not a straight line for the second-derivative operator.

OEM introduces an a priori constraint to improve the solution by setting $\sqrt{\alpha}\mathbf{L}(\mathbf{x}_a - \mathbf{x}_k) = \sqrt{\alpha}\mathbf{L}(\mathbf{x}_{\text{true}} - \mathbf{x}_k)$. Here, $\mathbf{L}$ is a Cholesky factorization of the a priori covariance matrix ($\mathbf{S}_a^{-1}$), where $\mathbf{S}_a^{-1} = \alpha\mathbf{L}^{\mathrm{T}}\mathbf{L}$ (Doicu et al. 2002). This stabilizes the solution around the a priori state-space vector $\mathbf{x}_a$. However, it produces a regularization error when the truth is not equal to the a priori. Our new regularization technique is based on the height derivative of the measurement, as shown later in this study, and thus, avoids this error.

First, we develop a stabilizer matrix ($\mathbf{L}$) at the kth iteration such as

$$\mathbf{L}_k = \begin{bmatrix} G_{k1}^h & -G_{k2}^h & 0 & 0 \\ 0 & G_{k2}^h & -G_{k3}^h & 0 \\ -- & -- & -- & -- \\ 0 & 0 & -G_{kn-1}^h & G_{kn}^h \end{bmatrix}, \tag{14}$$

where G_{k1}^h, G_{k2}^h, ... are the elements of the vector of $\mathbf{G}_k^h$. The vector $\mathbf{G}_k^h$ is calculated at the kth iteration using the Jacobian and the retrieved state-space parameter as $\mathbf{J}(\mathbf{x}_k)\mathbf{x}_k/\mathbf{x}_k$. The vector $\mathbf{G}_k^h$ is the linear slope of the object function. We construct the regularization matrix $\mathbf{L}_k$, by taking the finite-difference first derivative of $\mathbf{G}_k^h$ [Eq. (14)], which is equivalent to the one-dimensional Laplacian first-order derivative operator of the object function.

By definition the Laplacian operator is div{grad[$f(\mathbf{x})$]}. The expression grad[$f(\mathbf{x})$] is the slope of $f(\mathbf{x})$ along the direction where the individual measurement is minimizing the expression. A relation exists between two measurements along the altitude direction resulting from attenuation. The finite-difference divergence of the object function will, thus, also minimize the cost function in terms of the attenuation function. Now, we can equate the finite-difference first derivative of the object function, with $\mathbf{L}_k$ via $\Delta[\mathbf{y}_\delta - f(\mathbf{x}_k)] = \mathbf{L}(\mathbf{x}_{\text{true}} - \mathbf{x}_k)$. Here, Δ is the finite-difference first derivative:

$$\Delta[\mathbf{y}_\delta - f(\mathbf{x}_k)] = \left|[\mathbf{y}_\delta - f(\mathbf{x}_k)]\right|_{\text{zi}} - \left|[\mathbf{y}_\delta - f(\mathbf{x}_k)]\right|_{\text{zi}+1}, \tag{15}$$

where $|[\mathbf{y}_\delta - f(\mathbf{x}_k)]|_{\text{zi}}$ and $|[\mathbf{y}_\delta - f(\mathbf{x}_k)]|_{\text{zi}+1}$ are the residuals of the measurement at the ith and $(i + 1)$th altitude level, respectively. This process does not use the state-space parameters; it is based on the finite-difference derivative of the measurement, instead. This introduces an additional noise component to the retrieval. Our regularization must only reach an optimum reduction of the condition number of the inverted matrix.

b. Regularization strength

The RTLS method calculates the optimal regularization strength by considering the rightmost (i.e., lowest) eigenvalue of the matrix $\mathbf{W}$ (Koner and Drummond 2008a; Lampe and Voss 2007), with

$$\mathbf{W} = \mathbf{L}^{-\mathrm{T}}[\mathbf{J}^{\mathrm{T}}\mathbf{J} - g(\mathbf{x})\mathbf{I}]\mathbf{L}^{-1} \tag{16}$$

and $g(\mathbf{x}) = \|\mathbf{y}_\delta - \mathbf{J}\mathbf{x}\|^2/(1 + \|\mathbf{x}\|^2)$. A detailed discussion of Eq. (16) is beyond the scope of this paper but some considerations are opportune. The rightmost eigenvalue is the maximal Lagrange multiplier, which leads to the best solution in the Lagrangian multiplier method (Lampe and Voss 2008). Equation (16) determines the optimal regularization strength based on the norm value of the equivalent residual vector ($\mathbf{y}_\delta - \mathbf{J}\mathbf{x}$). The norm of the linearized residual vector is very much proportional to the different noise realizations associated with the pertinent problem. The lowest eigenvalue of $\mathbf{W}$ is high (low) when the value of $\|\mathbf{y}_\delta - \mathbf{J}\mathbf{x}\|$ is high (low) for the same $\mathbf{J}$ and $\mathbf{L}$ matrices. Thus, the optimal regularization strength is larger in the beginning of the iteration and decreases when the retrieved state vector approaches the true state vector. We have also improved the algorithm in such a way that high systematic measurement noise will not be realized as a signal by modifying the calculation of $g(\mathbf{x}) = \max[\|\mathbf{y}_\delta - f(\mathbf{x})\|^2/(1 + \|\mathbf{x}\|^2), \|\delta\|]$. The calculation of the regularization strength using RTLS implicitly uses an error criterion, which is very difficult to estimate explicitly in a nonlinear iterative process. The success of the retrieval is very often dependent on the choice of appropriate regularization strength for all iterations.

c. Error analysis

The determination of the retrieval error for a nonlinear iterative inverse solution is always difficult; however, a linear error and information content analysis can be done for simulated retrievals. If we assume that the numerical noise and the nonlinearity error at the last iteration are negligible, the retrieval error can be estimated (Koner and Drummond 2008b) using the values of α, $\mathbf{R}$, and $\mathbf{J}$ at the last iteration as

$$\|\text{error}\|^2 = \|(\mathbf{RKM} - \mathbf{I})\mathbf{x}\|^2 + \|(\mathbf{J}^{\mathrm{T}}\mathbf{J} + \alpha\mathbf{R})^{-1}\mathbf{J}^{\mathrm{T}}\|^2\langle\|\delta\mathbf{y}\|^2\rangle, \tag{17}$$

with $\mathbf{RKM} = (\mathbf{J}^T\mathbf{J} + \alpha\mathbf{R})^{-1}\mathbf{J}^T\mathbf{J}$ the regularized kernel matrix; and $\delta\mathbf{y}$ is the measurement noise. The information content in terms of the degrees of freedom (DFR) in the retrieval can be calculated as DFR = trace(**RKM**). Note that without regularization ($\alpha = 0$) the regularized kernel matrix is the identity matrix and DFR = dim(**x**).

4. Forward model

We now study a theoretical retrieval experiment for a nadir-pointing W-band (94 GHz) radar, in a configuration similar to the *CloudSat* cloud profiling radar (CPR). Our DRS retrieval results are compared with the OEM to gain confidence in the new technique. Similar to the procedure followed by L'Ecuyer and Stephens (2002), DSD variability, ice attenuation, and multiple scattering are not accounted for in this study. It should be pointed out that the ice/gas attenuation, eventually estimated by other measurements, can be subtracted from the total signal similar to the standard practice (Matrosov et al. 2008). Multiple scattering can play a role, especially in W-band radars [see, e.g., Battaglia et al. (2007, 2005) for discussions], but it can also be easily incorporated and does not pose a problem for the optimization method. We did not include it because a sufficiently fast code was not yet available. The DSD variability cannot be resolved using single measurements of CloudSat because of missing additional information. For the numerical simulation of CPR measurements we used 16 vertical range bins, each with a vertical thickness of 250 m. The measured range-dependent radar reflectivity is simulated by

$$Z_{\text{meas}} = \frac{\lambda^4}{4\pi^5|K|^2}\, e^{-2\int_0^r \kappa_{\text{ext}}(s)ds} \int \sigma_{\text{back}}(D)N(D)\, dD, \quad (18)$$

where λ is the radar wavelength, $K = (m^2 - 1)/(m^2 + 2)$ is the dielectric factor of the scattering target, m is the complex refractive index of the scatterer, and κ_{ext} is the volume extinction coefficient. The exponential factor accounts for the two-way attenuation along the slant path s of the radar beam. The quantity $N(D)\, dD$ denotes the number of particles with diameters between D and $D + dD$ in the target volume, where $\sigma_{\text{back}}(D)$ is the back-scattering cross section of a raindrop with diameter D, which we calculate using Mie theory. We made the simulations based on a drop-size distribution function of Marshall and Palmer (Marshall and Palmer 1948) for spherical raindrops:

$$N(D) = N_0 e^{-\lambda_{\text{sd}} D}, \quad (19)$$

with $\lambda_{\text{sd}} = 4.1(\text{RR})^{-0.21}$, RR the rain rate expressed in millimeters per hour, and $N_0 = 8 \times 10^6\ \text{m}^{-4}$ the number density at $D = 0$.

5. Results and discussions

We tested our retrieval algorithm using a hurricane simulation based on the Goddard Cumulus Ensemble-Cloud Resolving Model (GCE-CRM), which has been developed and improved at the National Aeronautics and Space Administration Goddard Space Flight Center (Tao and Simpson 1993). This simulation is also used for the Goddard profiling algorithm (GPROF; Olson et al. 1996) along with the OEM as a retrieval method. The database for the hurricane contains 15 000 rain-rate profiles, from which we have selected those with signals above the minimum detection level of *CloudSat* (-30 dBZ) and with a minimum rain-rate of 0.1 mm h^{-1}. This selection leaves us with 5688 profiles for the study. We assume a measurement noise of 1 dB for the simulated retrieval.

The a priori profiles for OEM retrievals are derived in L'Ecuyer and Stephens (2002) by solving for the rain-rate profiles using the Z–R and k–R relations, which are based on the Hitschfeld–Bordan algorithm (Hitschfeld and Bordan 1954). This is a plausible choice at the Ku band; however, as mentioned previously, this type of algorithm becomes extremely unstable when reverting to W-band radars and high rain rates. In these cases it is almost impossible to get information about the a priori in the presence of noise. To avoid huge a priori errors, we assume in this study a vertically constant 5 mm h^{-1} profile as a priori (and an initial guess as well).

a. Retrievals without constraints

The results using both DRS and OEM are shown in Figs. 1 and 2, respectively. The results of DRS outperform the OEM for all layers, except for the highest layer, where both perform equally well. The correlation coefficient and relative dispersion included in the figures are average values for four different bins of rain rates: 0–5, 5–15, 15–30, and above 30 mm h^{-1}. The relative dispersion is the standard deviation between the true and the retrieved rain rates, divided by the mean rain rate of the particular bin. The OEM does not capture the high rain rates for altitudes 1 and 0.5 km; they are always underestimated. The retrieval results using OEM at 0.5-km altitude are even negatively correlated, which indicates that no useful solution has been found. The average dispersion of the OEM retrievals significantly increases with decreasing altitude. For the DRS retrieval, the average relative dispersion at 0.5 km is

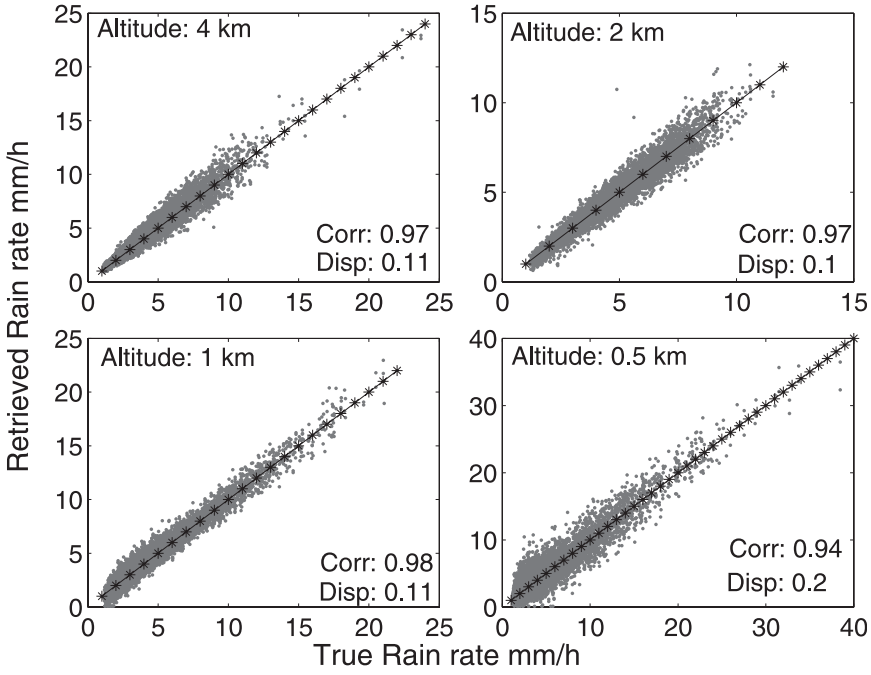

FIG. 1. Scatterplot of rain-rate retrieval using DRS for four different altitudes.

relatively high (0.2) in comparison with the other layers. Here, the DRS optimization more often fails to produce a good solution for low rain rates when the slope of the backscattering function is very high and the measurements close to the ground layer are strongly affected by attenuation.

To better understand our results, we analyze in more detail four critical profiles (Fig. 3). For each profile, we performed three Monte Carlo simulations by adding different noise patterns of 1 dB (~23%) to the simulated reflectivity profiles. Figure 3 contains the column average error (%), which is given by

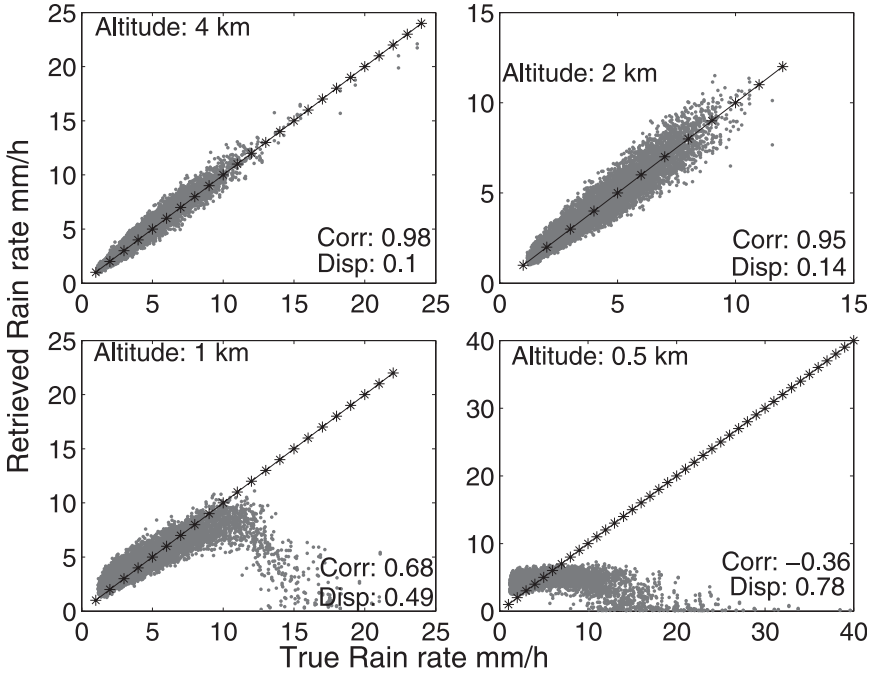

FIG. 2. Scatterplot of rain-rate retrieval using OEM for four different altitudes.

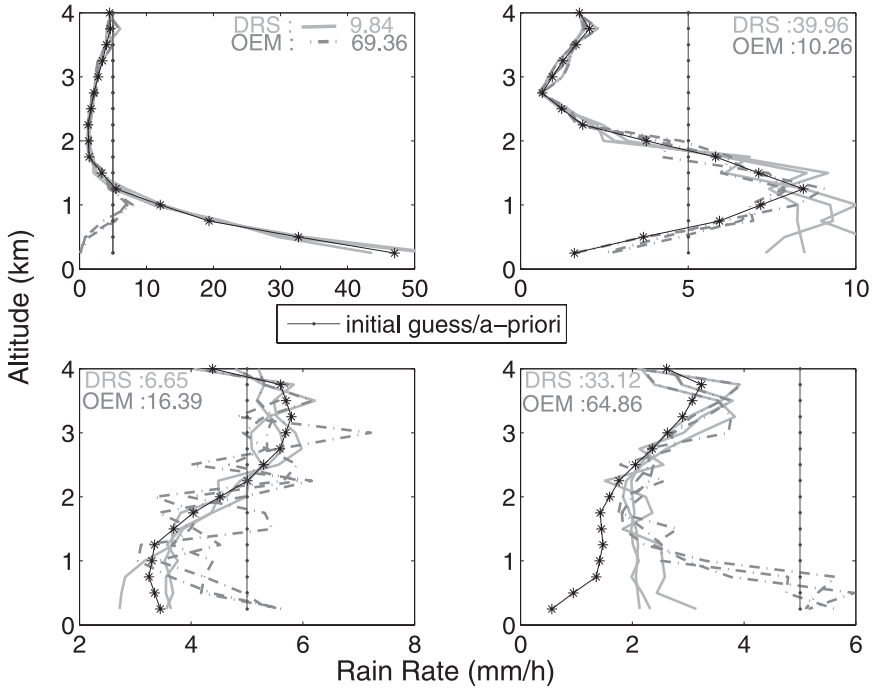

FIG. 3. Comparison of the retrievals for four different critical profiles using DRS and OEM.

$$\frac{\sum_{j=1}^{\text{nex}}\sum_{i=1}^{\text{ng}}\sqrt{(\mathbf{x}_{\text{rtv}}-\mathbf{x}_{\text{true}})^2}}{\text{nex}\sum_{i=1}^{\text{ng}}\mathbf{x}_{\text{true}}}, \tag{20}$$

with ng and nex as the number of grid points and experiments, respectively. The OEM solution of the profiles of 1, 3, and 4 are very poor, whereas the DRS solutions show higher stability in terms of the column average error. Only the column average error of profile 2, using the DRS, is higher than using the OEM; however, this is an artifact of the OEM: the a priori of OEM forces the lower part of the solution where the information from the measurement is very poor and corrupted by a high level of noise. The same OEM artifact makes the solution totally unacceptable for profile 1.

The reader might wonder whether the OEM does not reproduce the a priori of 5 mm h^{-1} at surface ranges, when attenuation diminishes the reflectivity to the noise level. According to the concept of the a priori information in the framework of the OEM, the a priori of 5 mm h^{-1} is expected to be retrieved when there is little or no information/signal at the surface. However, this is only true for monotonic functions, and here we are faced with a complex type of function. We can explain this behavior with the help of Fig. 3 (see profile 1). The a priori constraint forces the solution toward 5 mm h^{-1} when the rain rate is high and the Jacobian is ill conditioned. On the other hand, the optimizer minimizes the residual by redistributing the amount of backscattering and attenuation internally, which produces successive inappropriate retrieved state vectors in the intermediate steps in an iterative process. We can see that the effect of highly attenuationed component in the total signal, which would go with a high rain rate can be easily compensated by reducing the amount of the backscattering component. This forces the rain rate into smaller and smaller values.

It was expected that OEM provides a good solution for profile 3 because this profile is quite close to the a priori profile and within the range of a priori covariance. A significant oscillation, however, is observed because of the fact that the a priori covariance in conjunction with the error covariance is unable to optimally reduce the condition number of the inverted matrix and injects errors into the solution. It should be noticed that the bottom part of the solution of profile 3 converges to the given a priori. Both methods produce the wrong solution for profile 4, which will be discussed later.

Retrieval quality is often judged based on the information content in the retrieved result. Table 1 indicates, however, that the DFR is not necessarily a sound quality measure. Although the DFR of the OEM-(DRS)-based retrieved profile 1 (3) is almost equal to that of profile 2 (4), the two retrieved profiles show quite different

TABLE 1. Retrievals of information content DFR for the retrievals using OEM and DRS methods for four different profiles and three different experiments.

	Profile 1	Profile 2	Profile 3	Profile 4
DRS	8.49, 8.49, 8.82	9.58, 9.63, 9.57	6.41, 6.31, 6.40	6.44, 6.58, 6.38
OEM	14.4, 14.3, 14.4	14.1, 14.1, 14.1	13.8, 13.8, 13.8	14.5, 14.5, 14.4

column averaged errors. The OEM retrieved profiles are obviously of lower quality, although the DFR of profiles retrieved by OEM are much higher. For ill-posed inversion problems, it is mandatory to regularize the problem at the cost of information content. With no regularization applied, all the information may remain in the solution; however, the solution will generally not be acceptable because of the high retrieval error. In the OEM retrieval scheme, the a priori covariance matrix is assumed diagonal with variances of 25 $(\text{mm h}^{-1})^2$, which leads to a low regularization strength and keeps a high value of DFR. Low variance values in the a priori covariance lead to high regularization and the solution contains large biases. The DRS method, however, retrieves profiles with reasonable errors and a DFR just high enough to allow a sound solution to the problem, using a bias-free stabilizer and an appropriate regularization strength.

We mentioned the large discrepancy for profile 4, which can be explained considering the functional property of the problem. The measured reflectivity has two components: back scattering and attenuation (both components are functions of rain rate). These terms are opposite in sign. Such functions are sometimes called Lagrange-type functions. Attenuation is not only a function of the rain rate at a particular altitude but also of the rain rate of all altitudes above the considered level, which makes the present problem very complex especially for lower layers. The measured reflectivity values of the uppermost layers are dominated by the backscattering signal while attenuation is small. In such a situation, a gradient can be computed and any gradient search method or Newtonian iteration can produce a reliable solution. When moving downward in the profile attenuation increases and the reflectivity approaches zero. Thus, the backscattering signal and attenuation values become comparable. It is very difficult to construct a gradient in such situations and the gradient search method or Newtonian iteration fails to find a reliable search direction.

To better understand this problem, the measured reflectivity, the backscattering component, and the attenuation value for both the true and the retrieved rain rate using DRS for profile 4 are shown in Fig. 4. All three components of both profiles match well above 2 km. When the backscattering component and attenuation become comparable (below 2 km), the gradient-based search method fails to find a proper search direction; however, the least squares optimization optimizes the measured reflectivity within the noise level using inappropriate updating of the retrieved state vector. As a result, the retrieved profile at this region is higher than the truth. The higher values of both the backscatter component and the attenuation value compensate each other as they are of opposite sign. Thus, there are no reliable solutions if the measured reflectivity at the last layer is close to 0 (from 3 to -3 dBZ). The calculated reflectivity for about 15% of the profiles of our database is within the upper-mentioned range. It is also observed that the DRS can produce a reasonable retrieval in this group if the true profile is fairly constant at the lowest four layers. This can be explained by the regularization operator, which is supplying information from the height derivative measurements to solve these profiles. Even with a full DFR and with a no measurement noise, the gradient-based retrieval scheme cannot produce a unique solution in such a situation. Thus, the information content measure cannot guarantee a reasonable solution when the problem suffers in an iterative optimization process resulting from the functional complexity.

If the reflectivity values for the layers close to the ground are highly negative, an appropriate search direction can be determined and a reliable solution may be possible. In such a case, the attenuation values are much higher than the backscattering component and an appropriate search direction can be determined based on the dominating attenuation component. Accordingly, a reasonably good solution is achieved for profile 3 (Fig. 3), where the reflectivity values near the ground are close to -14 dBZ. The solution suffers, however, from the previous situation when the backscattering components largely decrease in the lowest four layers. The slope of the backscattering component is negative in such situations, as well as the slope of the attenuation. Thus, the least squares optimization adds the backscattering component to the attenuation value and produces a retrieved rain rate higher than the true one. For example, the retrieved profiles for profiles 2 and 4 (Fig. 3) are too high using DRS. A reliable solution can be produced, however, when the rain rate sharply increases for the last four layers (i.e., profile 1 in Fig. 3). There is also no problem in getting a reliable solution in this category, if the rain rate is fairly constant for the last four layers.

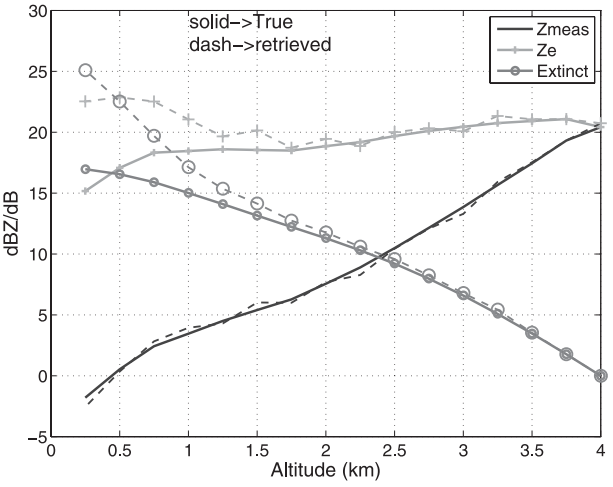

FIG. 4. Simulated measured radar reflectivity, backscattering component, and extinction of profile 4 (Fig. 3) for true and retrieved profiles.

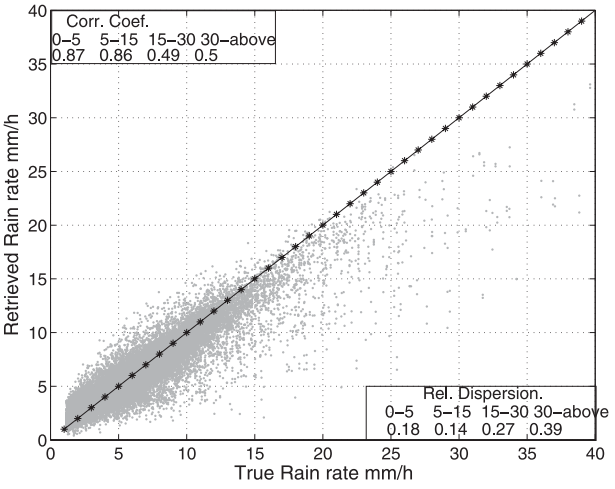

FIG. 5. Scatterplot of rain-rate retrieval using OEM under PIA constrained for all layers.

b. Retrieval with constraints

The functional property of the object function changes for a constrained retrieval. L'Ecuyer and Stephens (2002) introduced constraints like the liquid water path (LWP) to improve the retrievals. It can be argued that it may be difficult (or costly) to have another measurement collocated in both time and space, a necessity for the precipitating systems. The PIA estimates can, however, be obtained from the same radar measurement (e.g., by the surface reference technique); however, PIA can be estimated only over sea and homogeneous land surfaces—for example, like rain forests with sufficient accuracy. We investigated the effect of PIA as a constraint. The OEM retrievals with PIA improved considerably: the average correlation increases from 0.4 to 0.53 and the average dispersion decreased from 0.65 to 0.41. The average correlation of 0.53, however, is still very low and the retrievals above 10 mm h^{-1} are still not acceptable. This problem may arise from the assumed a priori profile of 5 mm h^{-1}. Thus, we extended the study using different a priori profiles and a priori covariance matrices. Based on the value of PIA, we have clustered the database into six classes with a PIA range of 0–5, 5–10, 10–15, 15–20, 20–25, and 25–30 dB. The mean rain rate and the diagonal of the variance of the rain rate of the individual groups are then used as a priori profile and a priori covariance matrix. The construction of the a priori profile and a priori covariance matrix are based on the truth; therefore, there are no guarantees of their validity for other databases or real measurements. The average correlation further improves to 0.68 and the average dispersion goes down to 0.27. The results contain, however, a bias (see Fig. 5), even though the problem is closely well posed (which will be discussed in the next paragraph). The biased results can be argued by the fact that the solution contains an error when the a priori profile is not equal to the truth, according to the basic assumption of OEM. The DRS solves the problem constrained with PIA uniquely neither using an a priori nor an a priori covariance matrix.

To better understand this behavior, we calculated the condition number of the Jacobians at the true rain rates with and without PIA constraints (Fig. 6). Obviously, the values of the condition number of the Jacobian are reduced by many orders of magnitude (ratio of $10^{12}-10^{15}$) because of the PIA constraint. The condition number of about 50% of the Jacobians under the PIA constraint is below 10. When the condition number of the Jacobian is around 10, any traditional nonlinear least squares can solve the problem. Thus, we have made a simulated retrieval using only the nonlinear least squares method (see Fig. 7). The statistical values of the retrieval without any regularization are slightly poorer than the improved OEM results but there is no bias. The average correlation is 0.64 for a nonlinear least squares case, whereas it is 0.68 for the OEM, and the average dispersions are 0.27 for both methods. The retrieval quality without any regularization (Fig. 7) is only degraded because of the fact that the condition number of 50% of the Jacobians is above 10 but below 10^3. In such situations regularization is needed to block the noise propagation from the inversion and measurement spaces to the state space. Thus, we use the DRS technique only when the condition number of the Jacobian is above 10. With this selection, we avoid unnecessary numerical computations and unwanted numerical noise, when the condition number of

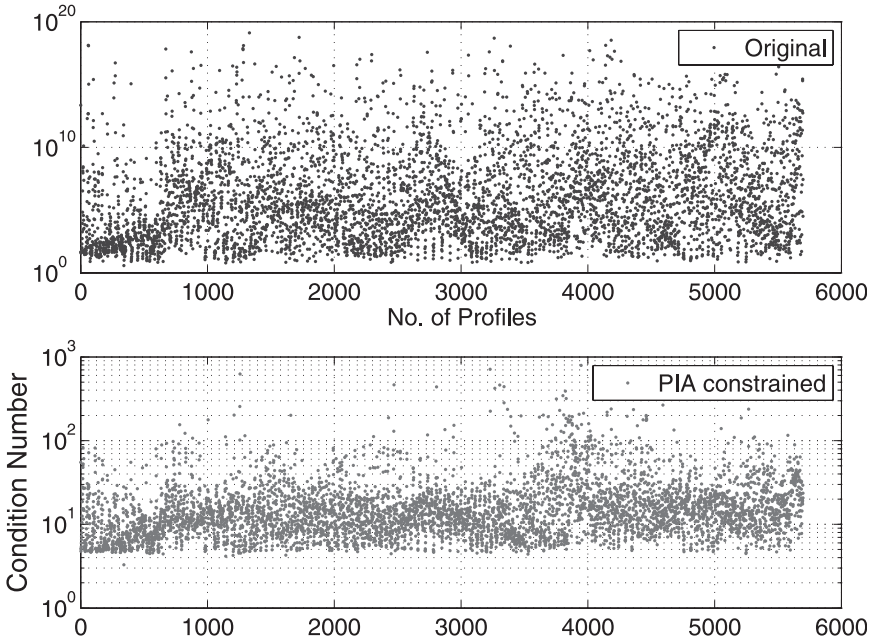

FIG. 6. The condition number of the Jacobians for true profiles without and with PIA constrained models.

the Jacobian is already low. This combination clearly produces the best results (Fig. 8): the average correlation coefficient is 0.89 and the average relative dispersion is 0.12, which indicates that the PIA constraint resolves for the functional complexity of the problem. These results are achieved because the new stabilizer does not inject any bias into the solution and the appropriate regulation strength is determined using the RTLS method.

The melting layer adds another uncertainty to the problem. The layer of melting hydrometeors, which is usually is 500–600 m thick in real situations (Kollias and Albrecht 2005), can contribute a substantial amount to PIA. Because the microphysical characterization of the melting layer is usually not sufficiently known, the PIA is uncertain even over oceans because it is difficult to separate the fractions due to rain and due to the melting layer. In addition, we have to consider the variability in the surface backscatter and the surface contamination of the lower 500 m. Our DRS methods lead to reasonable solutions down to 750 m without any constraints in such situations.

6. Conclusions

The retrieval using DRS is a promising technique for solving the problem of retrieving attenuated radar signals. The major strength of the DRS is its ability to find a global solution because it is based on the unbounded optimization technique. The evolutionary regularization binds the problem without disturbing the functional properties of the targeted situation. The DRS produces a bias-free solution because the regularization is based on the measurement space vector, instead of the state-space vector. Because the OEM is based on the bounded optimization technique, the results are dependent on the reliability of the boundary conditions or the supplied a priori information. The DRS does not require the covariance of the measurement noise and/or any a priori knowledge of the profile and/or the covariance of the state-space vector. Note that the DRS algorithm produces a global solution, not a global fit. We can also conclude that DRS, unlike the OEM, can solve the

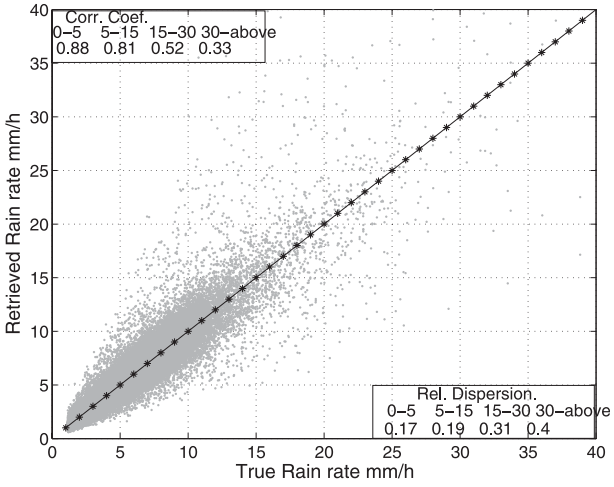

FIG. 7. Scatterplot of rain-rate retrieval using only nonlinear least squares under PIA constrained for all levels.

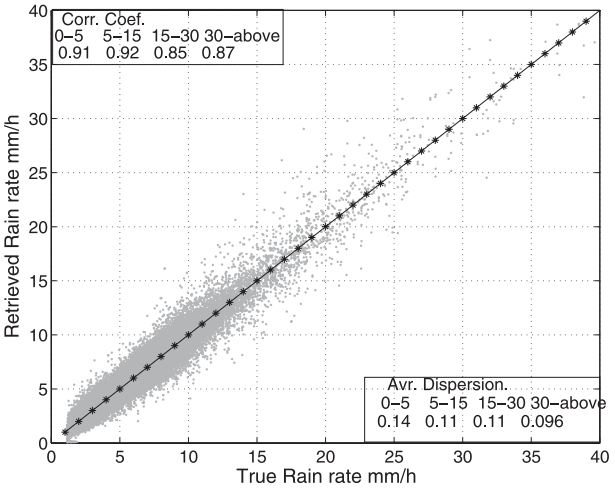

FIG. 8. Scatterplot of rain-rate retrieval using DRS under PIA constrained for all levels.

attenuating radar retrieval problem, even when additional constraints are not available.

We also conclude that the condition number of the Jacobian is an important parameter to understand ill-posed inversion problems. The information content in terms of DFR is not a reliable indicator of the retrieval quality for the type of problems considered here. Additional updating of the forward model—such as attenuation by ice–gases and multiple scattering effects—can be and will be incorporated into the present DRS algorithm.

Acknowledgments. This research has been supported by Deutsche Forschungsgemeinschaft (DFG) in the framework of the TOSCA project. The authors acknowledge Prof. J. R. Drummond of Dalhousie University, Canada, and Dr. S. Y. Matrosov of NOAA, for their useful discussions and suggestions. We also acknowledge the very helpful remarks of the anonymous reviewers, who considerably improved the readability of the text.

REFERENCES

Battaglia, A., M. O. Ajewole, and C. Simmer, 2005: Multiple scattering effects due to hydrometeors on precipitation radar systems. *Geophys. Res. Lett.,* **32,** L19801, doi:10.1029/2005GL023810.

——, ——, and ——, 2007: Evaluation of radar multiple scattering effects in *CloudSat* configuration. *Atmos. Chem. Phys.,* **7,** 1719–1730.

Ceccherini, S., 2005: Analytical determination of the regularization parameter in the retrieval of atmospheric vertical profiles. *Opt. Lett.,* **30,** 2554–2556.

Danzer, K., M. Otto, and L. A. Currie, 2004: Guidelines for calibration in analytical chemistry. *Pure Appl. Chem.,* **76,** 1215–1225.

Demoment, G., 1989: Image reconstruction and restoration: Overview of common estimation structures and problems. *IEEE Trans. Acoust. Speech Signal Process.,* **17,** 2024–2036.

Deufhard, P., H. Engl, and O. Scherzer, 1998: A convergence analysis of iterative methods for the solution of non-linear ill-posed problems under affinely invariant conditions. *Inverse Probl.,* **14,** 1081–1106.

Doicu, A., F. Schreier, and M. Hess, 2002: Iteratively regularized Gauss–Newton method for atmospheric remote sensing. *Comput. Phys. Commun.,* **148,** 214–236.

——, ——, and ——, 2003: Iteratively regularized Gauss–Newton method for bound constraint problems in atmospheric remote sensing. *Comput. Phys. Commun.,* **153,** 59–65.

——, ——, and ——, 2004: Iterative regularization methods for atmospheric remote sensing. *J. Quant. Spectrosc. Radiat. Transf.,* **83,** 47–61.

Gabella, M., A. Leone, and G. Perona, 1997: Aerosol profile variations retrieval through kernel functions in the oxygen absorption band at 762 nm. *Proc. Int. Geoscience and Remote Sensing Symp. 1997,* Singapore, China, Institute of Electrical and Electronics Engineers, 3–5.

Hanke, M., 1997: A regularizing Levenberg–Marquardt scheme, with applications to inverse groundwater filtration problems. *Inverse Probl.,* **13,** 79–95.

Hansen, P. C., 1998: *Rank-Deficient and Discrete Ill-Posed Problems: Numerical Aspects of Linear Inversion. SIAM Monogr. on Mathematical Modeling and Computation,* No. 4, Society for Industrial Mathematics, 247 pp.

Hitschfeld, W., and J. Bordan, 1954: Errors inherent in the radar measurement of rainfall at attenuating wavelengths. *J. Meteor.,* **11,** 58–67.

Hohage, T., 1997: Logarithmic convergence rates of the iteratively regularized Gauss-Newton method for an inverse potential and an inverse scattering problem. *Inverse Probl.,* **13,** 1279–1300.

Kollias, P., and B. A. Albrecht, 2005: Why the melting layer radar reflectivity is not bright at 94 ghz. *Geophys. Res. Lett.,* **32,** L24818, doi:10.1029/2005GL024074.

Koner, P., and J. Drummond, 2008a: Atmospheric trace gases profile retrievals using the nonlinear regularized total least squares method. *J. Quant. Spectrosc. Radiat. Transfer,* **109,** 2045–2059.

——, and ——, 2008b: A comparison of regularization techniques for atmospheric trace gases retrievals. *J. Quant. Spectrosc. Radiat. Transfer,* **109,** 514–526.

Lampe, J., and H. Voss, 2007: On a quadratic eigenproblem occurring in regularized total least squares. *Comput. Stat. Data Anal.,* **52,** 1090–1102.

——, and ——, 2008: Global convergence of RTLSQEP: A solver of regularized total least squares problems via quadratic eigenproblems. *Math. Modell. Anal.,* **13,** 55–66.

L'Ecuyer, T. S., and G. L. Stephens, 2002: An estimation-based precipitation retrieval algorithm for attenuating radars. *J. Appl. Meteor.,* **41,** 272–285.

Lhermitte, R., 1987: A 94-GHz Doppler radar for cloud observation. *J. Atmos. Oceanic Technol.,* **4,** 36–48.

Markovsky, I., and S. VanHuffel, 2007: Overview of total least-squares methods. *Signal Process.,* **87,** 2283–2302.

Marshall, J. S., and W. M. Palmer, 1948: The distribution of raindrops with size. *J. Meteor.,* **5,** 165–166.

Matrosov, S. Y., 2005: Attenuation-based estimates of rainfall rates aloft with vertically pointing Ka-band radars. *J. Atmos. Oceanic Technol.,* **22,** 43–54.

——, 2007: Potential for attenuation-based estimation of rainfall rate from CloudSat. *Geophys. Res. Lett.,* **34,** L05817, doi:10.1029/2006GL029161.

——, P. May, and M. Shupe, 2006: Rainfall profiling using atmospheric radiation measurement program vertically pointing 8-mm wavelength radars. *J. Atmos. Oceanic Technol.,* **23,** 1478–1491.

——, A. Battaglia, and P. Rodriguez, 2008: Effects of multiple scattering on attenuation-based retrievals of stratiform rainfall from cloudsat. *J. Atmos. Oceanic Technol.,* **25,** 2199–2208.

Olson, W., C. Kummerow, G. Heymsfield, and L. Giglio, 1996: A method for combined passive-active microwave retrievals of cloud and precipitation profiles. *J. Appl. Meteor.,* **35,** 1763–1789.

Riddell, C., I. Buvat, A. Savi, M. Gilardi, and F. Fazio, 2002: Iterative reconstruction of SPECT data with adaptive regularization. *IEEE Trans. Nucl. Sci.,* **49,** 2350–2354.

Rodgers, C. D., 2000: *Inverse Methods for Atmospheric Sounding: Theory and Practice.* World Scientific, 238 pp.

Rodriguez, G., 2005: An algorithm for estimating the optimal regularization parameter by the *l* curve. *Rend. Mat.,* **25,** 69–84.

Schimpf, B., and F. Schreier, 1997: Robust and efficient inversion of vertical sounding atmosphere high-resolution spectra by means of regularization. *J. Geophys. Res.,* **102,** 16 037–16 055.

Sima, D., S. VanHuffel, and G. H. Gloub, 2004: Regularized total least squares based on quadratic eigenvalue problem solver. *BIT Numer. Math.,* **44,** 793–812.

Steck, T., 2002: Methods for determining regularization for atmospheric retrieval problems. *Appl. Opt.,* **41,** 1788–1796.

——, and T. Clarmann, 2001: Constrained profile retrieval applied to the observation mode of the michelson interferometer for passive atmospheric sounding. *Appl. Opt.,* **40,** 3559–3571.

Su, M., F. Xua, X. Cai, K. Renb, and J. Shen, 2007: Optimization of regularization parameter of inversion in particle sizing using light extinction method. *China Particuol.,* **5,** 295–299.

Sun, A., H. Tang, and G. Yuan, 2007: Determination of the particle size range in the visible spectrum from spectral extinction measurements. *Meas. Sci. Technol.,* **18,** 3572–3582.

Tao, W. K., and J. Simpson, 1993: Goddard Cumulus Ensemble Model. Part I: Model description. *Terr. Atmos. Ocean. Sci.,* **4,** 35–72.

Tsai, C. L., and W. W. Kao, 2006: Ill-conditioned GPS compass attitude determination using regularization approach. *Appl. Math. Comput.,* **183,** 184–198.

VanHuffel, S., and J. Vandewalle, 1991: *The Total Least Squares Problems: Computational Aspects and Analysis.* Vol. 9, *Frontiers in Applied Mathematics,* SIAM, 300 pp.

Vasco, D. W., 1997: Groups, algebras, and the non-linearity of geophysical inverse problems. *Geophys. J. Int.,* **131,** 9–23.

Veselovskii, I., A. Kolgotin, V. Griaznov, D. Muller, U. Wandinger, and D. Whiteman, 2002: Inversion with regularization for the retrieval of tropospheric aerosol parameters from multiwavelength lidar sounding. *Appl. Opt.,* **41,** 3685–3699.

Wang, Y., and Y. Yuan, 2005: Convergence and regularity of trust region methods for nonlinear ill-posed inverse problems. *Inverse Probl.,* **21,** 821–838.